

2016

Modeling Early Stage Bone Regeneration With Biomimetic Electrospun Fibrinogen Nanofibers and Adipose-Derived Mesenchymal Stem Cells

Michael P. Francis

Yas M. Moghaddam-White

Patrick C. Sachs


Old Dominion University, psachs@odu.edu

Matthew J. Beckman

Stephen M. Chen

See next page for additional authors

Follow this and additional works at: https://digitalcommons.odu.edu/medicaldiagnostics_fac_pubs

 Part of the [Biomedical Commons](#), [Biomedical Engineering and Bioengineering Commons](#), and the [Medical Biotechnology Commons](#)

Repository Citation

Francis, Michael P.; Moghaddam-White, Yas M.; Sachs, Patrick C.; Beckman, Matthew J.; Chen, Stephen M.; Bowlin, Gary L.; Elmore, Lynne W.; and Holt, Shawn E., "Modeling Early Stage Bone Regeneration With Biomimetic Electrospun Fibrinogen Nanofibers and Adipose-Derived Mesenchymal Stem Cells" (2016). *Medical Diagnostics & Translational Sciences Faculty Publications*. 30.
https://digitalcommons.odu.edu/medicaldiagnostics_fac_pubs/30

Original Publication Citation

Francis, M. P., Moghaddam-White, Y. M., Sachs, P. C., Beckman, M. J., Chen, S. M., Bowlin, G. L., . . . Holt, S. E. (2016). Modeling early stage bone regeneration with biomimetic electrospun fibrinogen nanofibers and adipose-derived mesenchymal stem cells. *Electrospinning*, 1(1), 10-19. doi:10.1515/esp-2016-0002

Authors

Michael P. Francis, Yas M. Moghaddam-White, Patrick C. Sachs, Matthew J. Beckman, Stephen M. Chen, Gary L. Bowlin, Lynne W. Elmore, and Shawn E. Holt

Research Article

Open Access

Michael P. Francis, Yas M. Moghaddam-White, Patrick C. Sachs, Matthew J. Beckman, Stephen M. Chen, Gary L. Bowlin, Lynne W. Elmore, and Shawn E. Holt*

Modeling early stage bone regeneration with biomimetic electrospun fibrinogen nanofibers and adipose-derived mesenchymal stem cells

DOI 10.1515/esp-2016-0002

Received Jun 12, 2015; revised Jan 08, 2016; accepted Jan 13, 2016

Abstract: The key events of the earliest stages of bone regeneration have been described *in vivo* although not yet modeled in an *in vitro* environment, where mechanistic cell-matrix-growth factor interactions can be more effectively studied. Here, we explore an early-stage bone regeneration model where the ability of electrospun fibrinogen (Fg) nanofibers to regulate osteoblastogenesis between distinct mesenchymal stem cells populations is assessed. Electrospun scaffolds of Fg, polydioxanone (PDO), and a Fg:PDO blend were seeded with adipose-derived mesenchymal stem cells (ASCs) and grown for 7–21 days in osteogenic differentiation media or control growth media. Scaffolds were analyzed weekly for histologic and molecular evidence of osteoblastogenesis. In response to osteogenic differentiation media, ASCs seeded on the Fg scaffolds exhibit elevated expression of multiple genes associated with osteoblastogenesis. Histologic stains and scanning electron microscopy demonstrate widespread mineralization within the scaffolds, as well as *de novo* type I collagen synthesis. Our data demonstrates that electrospun Fg nanofibers support ASC osteogenic differentiation, yet the scaffold itself does not appear to be osteoinductive. Together, ASCs and Fg recapitulate early stages of bone regeneration *ex vivo* and presents a prospective autologous therapeutic approach for bone repair.

Keywords: fibrinogen; adipose-derived mesenchymal stem cell; electrospinning; bone regeneration; osteoblastogenesis

1 Introduction

Healing of a fractured bone in the body occurs through distinct yet overlapping stages (Table 1) [1], the first of which is the *early inflammatory stage* where a fibrin-laced hematoma develops within the fracture. This hematoma clot originates from lacerated blood vessels in the bone and periosteum. Hematoma formation leads to the infiltration of inflammatory cells (macrophages, monocytes, and lymphocytes) and osteoblasts to clean and resorb the necrotic bone and inflamed hematoma. Granulation tissue develops from cells of the periosteum and endosteum as the hematoma is resorbed, followed by an infiltration of mesenchymal stem cells (MSCs) into the granulation tissue to begin repairs, including new collagen deposition [2]. In the next stage of healing, *the repair stage*, the progenitor cells differentiate into chondrocytes and later osteocytes, which can be recognized by the upregulation of common bone-specific marker genes and proteins, such as osteocalcin, osteopontin, Runx2, and bone sialoprotein protein [3]. Recruited fibroblasts further deposit a mesh of connective tissue to support vascular ingrowth into the granulation tissue, with a collagen matrix supporting the osteoid. A soft callus structure ultimately forms around the repair site that fills with woven bone made by the osteoblasts. Fracture healing concludes in the *late remodeling stage*, where healing bone regains its original structures and mechanical integrity.

Though fracture healing usually progresses smoothly, non-unions in bone are prevalent when regeneration fails. To accelerate bone healing or the closure of non-unions,

Michael P. Francis, Lynne W. Elmore: Department of Pathology, School of Medicine at Virginia Commonwealth University

Yas M. Moghaddam-White: Department of Biomedical Engineering, Virginia Commonwealth University

Patrick C. Sachs: Department of Human and Molecular Genetics, Virginia Commonwealth University, Richmond, VA; Department of Medical Diagnostic & Translational Sciences, Old Dominion University, Norfolk, VA

Matthew J. Beckman: Genetworx, LLC, Glen Allen, VA

Stephen M. Chen: Bon Secours-St. Mary's Hospital, Richmond, VA

Gary L. Bowlin: Department of Biomedical Engineering, University of Memphis, TN

***Corresponding Author: Shawn E. Holt:** Department of Natural Science, Richard Bland College of the College of William & Mary, Petersburg, VA; Email: seholt@rbc.edu; Tel.: 804-862-6100, ext. 9811



Table 1: Bone Remodeling During Healing

Early-Stage Bone Regeneration Events [#]	Bone Regeneration Model
Hematoma formation (fiber diameter dependent upon physiological conditions regulating fiber assembly, with 80–458 nm diameters reported)	Electrospun fibrinogen with 364±142 nm fiber diameter (n = 50, mean ± SD)
White cells and osteoblasts infiltrate and clear clot in ~7–14 days	MG63 osteoblasts dissociate electrospun fibrinogen scaffolds in 4–9 days (Fig. 2F)
Type I collagen deposition and ECM remodeling	ASCs (and fibroblasts)* remodel electrospun fibrinogen with collagen (Fig. 2)
Osteoblastogenesis occurs initially from MSCs of periosteum (pericyte) origin, not from bone marrow MSCs (BMSCs)	ASCs (putative pericyte origin), but not BMSC, differentiate into osteoblasts on electrospun fibrinogen nanofibers (Fig. 2–5)
Bone-specific ECM (<i>e.g.</i> osteocalcin & collagen type I) deposited by osteoblasts in a mineralized matrix	ASCs in osteogenic conditions remodel electrospun fibrinogen scaffold with collagen, osteocalcin, and mineralized matrix (Fig. 2–4, 6)

[#]Adapted summary from [3]; *Adapted from [27]

some health care providers have recently implemented injecting a basic fibrinogen (Fg) gel for guiding osteogenesis into the fracture, both with and without MSCs added to the mixture [4]. This and other studies indicate high variability in the results, with an excess of Fg injection seen to inhibit new bone formation in controlled clinical studies [4–11]. Further, the form of the Fg [5–8] and the type of MSC used [5–11] appear to be critical aspects to successful bone healing *in vivo* and for modeling osteoblastogenesis *in vitro*.

While bone marrow-derived MSCs (BMSCs) have been the most widely studied of the MSC types, the existence of analogous adipose-derived mesenchymal stem cells (ASCs) in human fat have gained considerable interest [12, 13], in part due to sharing a very similar transcriptome, and a nearly identical immunophenotype [14] and differentiation potential [12–16] with BMSCs. ASCs are up to 1,400 times more abundant and are a more readily accessible cell source relative to BMSCs [15, 16]. Additionally, ASCs have been shown able to restore lethally irradiated bone marrow and fully repopulate the hematopoietic system [17], revealing the potential for allogeneic ASC transplantation. Furthermore, ASCs, as with MSCs from other tissue sources, secrete numerous growth factors implicated in tissue development and regeneration [18]. As progenitor cells of a perivascular origin (such as in the periosteum) are major contributors to primary bone healing, the putative pericyte origin for ASCs, as well as their association with a perivascular niche [19–23], suggests a role for ASCs as a model for osteoblastogenesis.

In tissue engineering, electrospinning has rapidly gained interest due to its numerous advantages over con-

ventional scaffold fabrication methods [24] for use as a matrix for *in vitro* 3-dimensional (3D) cell-based experiments. Natural matrix materials, such as collagen, laminin, elastin, and Fg, with or without supporting synthetic blends (polydioxanone (PDO) or polyethylene glycol (PEG)), can be electrospun into scaffolds of nearly any size, shape, or microscopic properties [24–28]. Unlike conventional polymer processing techniques, electrospun scaffolds can closely resemble native extracellular matrices in geometry, fiber size, and material composition.

There are numerous practical and biologic reasons for using Fg to model bone regeneration. Fg is an integrin-spanning glycoprotein that binds collagen, fibrin, and heparin sulfate, and has been used clinically for a variety of applications for more than 60 years [29, 30]. Fg is an extracellular matrix (ECM) derivable protein, is easily purified from human specimens [4], and is well suited for electrospinning [27, 31–33]. Fg binds basic fibroblast growth factor (bFGF) and vascular endothelial growth factor (VEGF) with high affinity; both bFGF and VEGF potentiate endothelial cell proliferation and may contribute to the healing response. ASCs express high levels of bFGF and VEGF, as well as many other pro-angiogenic factors [14], again supporting the pairing of ASCs and Fg to model bone regeneration.

Addressing a need for generating bone for pre-clinical testing and for potential therapeutic purposes, we explore the feasibility of using electrospun Fg to support osteoblastogenesis in donor-derived ASCs. Using quantitative RT-PCR (qRT-PCR), immunologic and histologic staining procedures, and confocal and electron microscopy, we show ASCs together with electrospun Fg recapitulate key

events in early bone regeneration, thus providing an attractive pre-clinical model for bone regenerative medicine-related applications.

2 Materials and Methods

2.1 ASC Primary Isolation and Culture

ASCs were procured from donors as we described previously [34, 35] and in accordance with Virginia Commonwealth University's Institutional Review Board. Briefly, lipoaspirate was obtained as surgical waste from patients undergoing elective, cosmetic surgery. Around 250 ml of fat was extensively washed in PBS then digested for 1 hr in 0.1% collagenase A (Sigma-Aldrich) solution with shaking at 37°C. The digested tissue was centrifuged for 10 min at 200 xg, with the floating adipocytes and media aspirated off and the remaining pellet incubated for 10 min in 140 mM ammonium chloride (Sigma-Aldrich) red blood cell lysis buffer. The cells were filtered through 100µm and 40µm mesh filters (BD Bioscience) and gradient separated for mononuclear cells (Histopaque, Sigma-Aldrich). Cells were plated on plastic in low glucose DMEM (Invitrogen) with 30% fetal bovine serum (FBS) (Hyclone) and 1% antibiotic/antimycotic (ABAM; penicillin-streptomycin-gentamicin, Invitrogen) overnight. The next day, non-adherent cells were washed-off with PBS to select for the adherent MSC population. The cells were cultured in low glucose DMEM with 10% FBS, and 1% ABAM, known as basic ASC growth media. Adherent cells were expanded and then confirmed by flow cytometry to exhibit the MSC immunophenotype and by histology and qRT-PCR to display tri-lineage mesenchymal differentiation potential, as previously described [34, 35].

2.2 BMSCs, BJ Fibroblasts, and MG63 Cell Culture

Human foreskin fibroblasts (BJ) were obtained from ATCC (Manassas, VA) and expanded in D9C media (DMEM, 1X Medium 199, 10% CCS (Cosmic Calf Serum, Hyclone)) and 1% ABAM. MG63 osteosarcoma cells (ATCC) were cultured in basic ASC growth media or specific differentiation media. Two BMSC strains were obtained from the iliac crest of healthy human patient donors in accordance with the VCU's IRB, using standard isolation procedures [36]. BMSCs and ASCs were maintained in low glucose DMEM supplemented with 10% FBS, 15ng/mL bFGF (Sigma-Aldrich),

and 1% ABAM. All cells were incubated at 37°C and 5% CO₂. BJ fibroblasts, due to their inability to differentiate along multiple mesenchymal lineages, provided a negative cell strain of mesenchymal origin to directly compare with ASCs. BMSCs and MG63 human osteosarcoma cells served as a positive control for bone-specific markers.

2.3 Electrospinning Fg, PDO, and Fg:PDO

Solutions of lyophilized bovine Fg (Fraction 1, Type 1-S from bovine plasma, Sigma Aldrich) were made with a 10% (by volume) 10X minimal essential medium (MEM, Sigma Aldrich) and 90% 1,1,1,3,3,3 hexafluoro-2-propanol (HFP; TCI America, Portland, OR) at concentrations of 100 mg/mL (ratio determined to make biomimetic fiber diameters as described in our prior work [37]), and allowed to dissolve overnight with shaking. Solutions of PDO (Ethicon, Somerville, NJ) were made at 100 mg/ml concentrations, dissolved in HFP overnight with shaking at room temperature (RT). Fg:PDO blended scaffolds were combined in one vial after mixing overnight with an additional 10% MEM to allow the polymers to stay in solution to effectively electrospin. The solution was electrospun to create non-woven, randomly oriented fibrous mats. The electrospinning apparatus consisted of a syringe pump (KD Scientific), high voltage power supply (Spellman CZE1000R, Spellman High Voltage Electronics Corp.), 10 ml syringes (BD Bioscience) with 18-gauge blunt-end needle, and a 303 stainless steel mandrel (typically at 10.2 cm length × 2.5 cm width × 0.3 cm thick) used as a rotating collection target. Electrospinning parameters were typically constant at 30 kV-applied voltage, 12.5 cm distance between the needle and grounded mandrel, 2.5 mL/hour solution dispensing rate, a 2 cm/s translational speed over a 7 cm throw, and 500 RPM rotation speed, as we reported previously [44]. The scaffolds were disinfected in 80% ethanol and washed in PBS with 10 mm discs formed using tissue biopsy punches for subsequent cell seeding. ImageJ64 (NIH shareware) was used on scanning electron microscopic (SEM) images to determine the average (mean) fiber diameter from random fibers (n = 50), from scaffolds left in culture media at 37°C for 7 days.

2.4 Scaffold Cell Seeding and Culture

To reduce donor-specific differences that may exist in ASCs, the low passage (population doubling 2–8) strains were pooled for seeding on scaffolds. A concentrated 100 µl drop of 50,000 cells (500 cells/µl) was carefully

placed on the center of the 10 mm electrospun discs for each experimental condition. Cells were allowed to adhere in the incubator for 15 min and then 500 μ l of osteogenic differentiation media (high glucose DMEM, 10% FBS, 0.1 μ M dexamethasone, 50 μ M ascorbate-2-phosphate, 10 mM β -glycerophosphate, 1% ABAM) or control media (osteogenic media without dexamethasone) was then added. Cellularized scaffolds were cultured in ASC growth media or osteogenic media at 37°C and 5% CO₂, with media changed every 2–3 days. Scaffolds were collected at days 1, 7, 14, and 21, fixed, and processed as described below.

2.5 Quantitative Real Time RT-PCR

Total cellular RNA was extracted from electrospun tissue-analogues using Trizol[®] Reagent (Invitrogen) according to manufacturer's protocol. For adequate RNA yield, five cell-seeded 10 mm scaffolds were homogenized for each condition and pulverized together with a tissue grinder in 1ml of Trizol. RNA concentrations and purity were estimated on a nanodrop spectrophotometer (Thermo Scientific, Waltham, MA). RNA was reverse transcribed using a random hexamer and the SuperScript First Strand Synthesis System (Invitrogen). An ABI PRISM 7900 (Life Technologies) was used for gene expression (qRT-PCR) analysis from quintuplicate samples. Primers for 18S (ABI standard sequences [35]), osteocalcin (Fwd: 5'-AGCAAAGGTGCAGCCTTTGT-3'; Rev: 5'-GCGCCTGGGTCTCTCACT-3'; TaqMan probe: 5'-CCTCGCTGCCCTCCTGCTTGG-3'), RUNX2 (Fwd: 5'-CCCGTGGCCTTCAAGGT-3'; Rev: 5'-CGTTACCCGCCATGACAGTA-3'; TaqMan probe: 5'-CCACAGTCCCATCTGGTACCTCTCCG-3'), and alkaline phosphatase (Fwd: 5'-GCACTCCCACTTCATCTGGAA-3'; Rev: 5'-GAAACCAATAGGTAGTCCACATTG-3'; TaqMan probe: 5'-CGCACGGAACCTCCTGACCCTTGAC-3') were used. Relative expression levels for the lineage specific genes were calculated using standard curves generated from the triplicate dilution series of the cDNA with normalization to the 18S housekeeping gene.

2.6 Histological Scaffold Processing and Evaluation

Scaffolds were washed with PBS and fixed in 10% formalin, cryosectioned or paraffin embedded to section, and mounted for standard histological hematoxylin and eosin (H&E), Ki67 immunohistochemistry, and Masson's Trichrome staining (VCU Clinical Pathology Research Ser-

vices). Ethanol-fixed samples were paraffin embedded and routinely processed for Alizarin Red S staining [12, 43, 46]. Slides were visualized by phase and fluorescence microscopy. For osteocalcin immunolabeling, cells were washed with PBS and fixed with 3.7% paraformaldehyde for 30 min, and then permeabilized with 0.5% Triton X-100 for 10 minutes. Following PBS washing, cells were blocked with 4% bovine serum albumin (BSA) or normal goat serum in PBS for 1 hour, and then incubated in 4% BSA/goat serum in PBS with a polyclonal antibody for osteocalcin (100 μ g/ml, Santa Cruz Biotechnology) overnight at 4°C in a humidified chamber. After PBS washes, cells were incubated 4% BSA in PBS with Alexa-Fluor 488 goat anti-rabbit IgG (1:200 dilution; Invitrogen) for 1 h at RT. Cells were stained 4',6-diamidino-2-phenylindole (DAPI) upon mounting in Vectashield (Vector Lab H-1000).

2.7 Microscopic Scaffold Evaluation

For SEM evaluation, scaffolds were fixed in 50% glutaraldehyde and processed by standard methods with gold sputter coating prior to analysis by a Zeiss EVO 50 XVP (Nano Technology System Division, Carl Zeiss). For confocal microscopy, cells were grown on scaffolds in chambered coverglass, or prepared from paraffin-embedded scaffold sections mounted on slides. A Leica TCS-SP2 AOBs confocal laser-scanning microscope was used to capture images using identical light intensity settings, using Leica LCSLite imaging software. Phase and fluorescent images were captured on an Olympus BX51 with Q-Capture Pro using identical light intensity settings.

2.8 Statistical Analyses

Cell numbers and the percentage of positively immunostained cells were based on 5 randomly selected microscopic fields, from on average of 4 different sections. An ImageJ64 cell counter tool was used to assist with the generation of quantitative data. Statistical analysis for cell counts, percent immunopositivity, and qPCR gene expression comparisons were performed using a one-way ANOVA followed by a Tukey's test for pairwise comparison with the *a priori* significance set at $p < 0.05$.

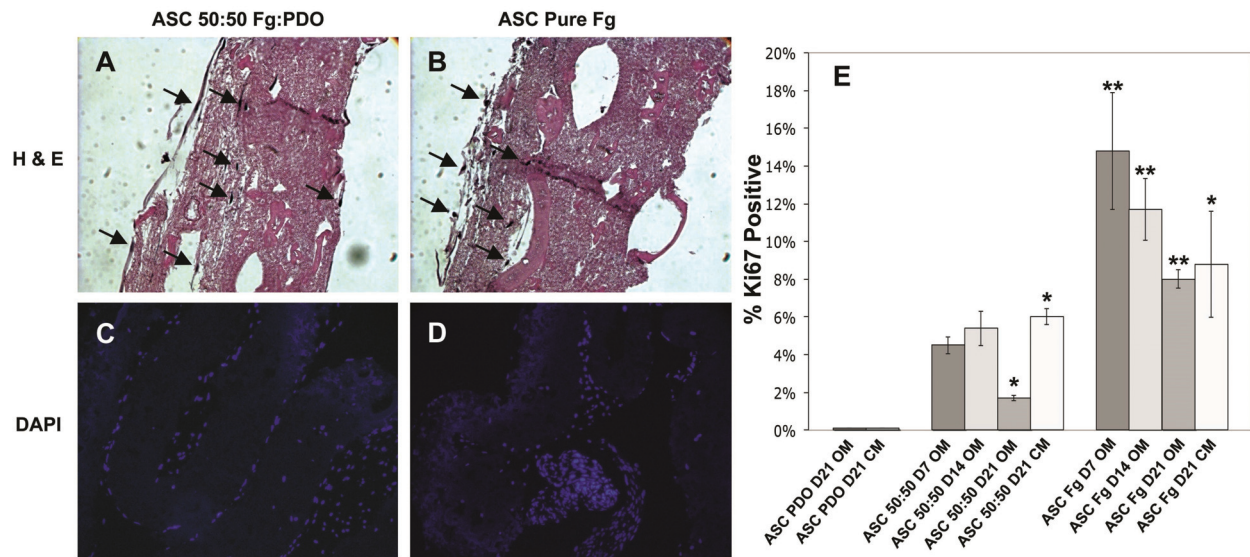


Figure 1: Electrospun Fg:PDO and Fg Scaffolds Support ASCs. ASCs seeded on electrospun 50:50 Fg:PDO (A&C) or Fg (B&D) show cells present throughout the constructs at 2 weeks of culture, as assayed by H&E (A&B) and DAPI (C&D) (20× magnification). Ki67 staining of ASCs grown on electrospun Fg:PDO, pure Fg, and PDO was performed (E), with the percent of positive staining, replicative cells quantitated from 5 random fields. Cells were grown in either osteogenic media (OM) or control media (CM) for 7–21 days (D7, D14, D21) as indicated, and a minimum of 4 independently seeded scaffolds were analyzed for each assay. *indicates statistical significance at $p < 0.05$ using one-way ANOVA vs. PDO scaffolds, and **indicates $p < 0.05$ vs. both PDO and Fg:PDO scaffolds. Arrows indicate cell growth on the matrix.

3 Results

ASC Attachment and Proliferation on Electrospun Fg Scaffolds

To assess cell attachment, viability, proliferative index, and penetration into electrospun Fg and Fg:PDO scaffolds, 5×10^5 ASCs were seeded on scaffolds and collected every 7 days for DAPI, H&E, and Ki67 immunostaining. We previously reported that crosslinking Fg by various methods leaves the scaffold impermeable to cells [37]; therefore, scaffolds were left in their native, uncrosslinked state after electrospinning. As shown in Figure 1, viable ASCs were abundantly present on pure Fg scaffold (panel B) with a modest reduction in cellularity on blended Fg:PDO scaffolds (panel A) after 2 weeks in culture. Of note, the number of cell layers formed on/within the electrospun PDO, Fg:PDO, and pure Fg scaffolds was clearly distinct: for pure PDO scaffolds, there was a single-cell layer of ASCs on the periphery with no detectable cells penetrating the interior (data not shown); for the blended Fg:PDO scaffolds, ASCs typically formed layers comprising 4–5 cells thick with some cells infiltrating deeper into the scaffold (Figure 1A); for pure Fg scaffolds, cells formed thick layers (averaging 8–12 cells deep) with many cells penetrating beyond the surface of the scaffold (Figure 1B). H&E

stained scaffolds were also used to compare the cellularity in the blended Fg:PDO (Figure 1C) and pure Fg scaffolds (Figure 1D). A 2.5–4-fold increase in ASC number was seen in Fg:PDO and Fg scaffolds as compared to pure PDO scaffolds (Figure 1E).

Using Ki-67 as a marker to assess proliferative indices, we show that on average 9% of undifferentiated ASCs (control media, CM) proliferate on pure Fg scaffold, and on average 6% of undifferentiated ASCs proliferate on the Fg:PDO blend after 3 weeks in culture (Figure 1E). As expected for cells undergoing differentiation, ASCs when cultured in osteogenic media (OM) exhibited a trend for reduced proliferation overtime in culture (Figure 1E), a pattern highly consistent with scaffold cellularity shown in Figure 2. Of the three materials tested, the pure PDO scaffold was substantially inferior to supporting the viability or growth of ASCs as shown by Ki-67 staining in Figure 1E.

New Extracellular Matrix Production and Remodeling By ASCs

Masson Trichrome histochemical staining revealed the ability of ASCs to deposit new ECM. We find that ASCs were able to remodel the Fg scaffolds over time, depositing new collagen in place of Fg from 1 to as many as 10 weeks of culture, in both pure electrospun Fg and Fg:PDO (Figure 2).

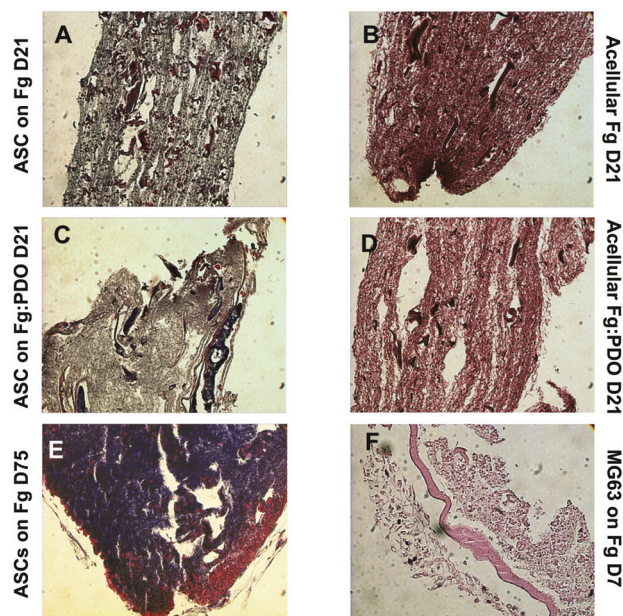


Figure 2: Histology of ASCs and MG63s on Electrospun Fg Matrix. Masson's Trichrome stains of ASCs in osteogenic differentiation media grown on electrospun Fg for 21 (A) and 75 days (E) show pronounced Masson's Trichrome staining (blue for collagen) relative to an acellular control in media for 21 days (B). Fg:PDO blend similarly showed new collagen deposition at 21 days of ASC differentiation (C), as compared to an acellular Fg:PDO control at day 21 (D). H&E staining of MG63s on electrospun Fg for 7 days shows a dissociated yet densely cellular scaffold (F). Magnification was 20 \times .

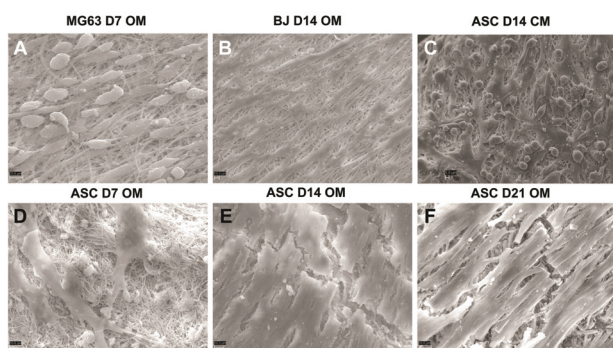


Figure 3: Topography of Bone-Induced ASCs on Electrospun Fg Scaffolds. MG63 osteosarcoma cells are shown by SEM at day 7 on electrospun Fg as an osteoblast reference (A). BJ fibroblasts in osteogenic differentiation media (OM) (B) and ASCs grown in control growth media (CM) (C) on Fg scaffolds for 14 days are shown for reference. ASCs maintained in OM are shown at 7–21 days of differentiation (D–F) via SEM (at 2000 \times magnification), showing a unique morphology on the scaffold surface, distinct from ASCs in CM. Qualitatively, the scaffolds in (D–F) were very brittle.

Contrary to previous data with fibroblast cultures on electrospun Fg, ASCs seem to naturally adhere to the electrospun Fg (Figure 2A and 2C) and allow extended culture on associated 3D scaffolds (up to 75+ days (Figure 2E)). In

contrast, the histology of MG63 cells grown on electrospun Fg for 7 days shows a completely dissociated matrix (Figure 2F).

ASCs Mineralize Electrospun Fg

To assess changes in scaffold surface topography during osteogenic differentiation with control or ASCs seeded on electrospun Fg-containing and PDO scaffolds, we performed SEM of the bone-induced (osteogenic media (OM)) and control media (CM) samples for up to 21 days. Compared to acellular (not shown), MG63- or BJ-seeded Fg scaffolds (Figure 3A and 3B, respectively), and ASCs on PDO (not shown), only the differentiating ASC-containing scaffolds exhibited a significant change in morphology and topography (Figure 3D–3F), with features suggestive of scaffold mineralization. This mineralization-like change in electrospun scaffold surface topography is consistent with previous findings from our collaborators using a chemical mineralization protocol [38] and is in stark contrast to the Fg scaffolds cellularized with ASCs that are maintained in control media for 2 weeks (Figure 3C) or for longer periods of time (up to 5 weeks; not shown).

In order to evaluate the potential of ASCs seeded on electrospun Fg to form mature bone-like material, we assayed for calcification using Alizarin Red S (ARS) staining of ASCs seeded on Fg, Fg:PDO and pure PDO scaffolds seeded up to 21 days after osteoinduction (Figure 4). While pure PDO scaffolds with ASCs showed a marked absence of staining (Figure 4A), matrix mineralization was clearly detected for Fg:PDO (Figure 4B) and with pure Fg scaffolds at day 21 (Figure 4F), with staining appearing to intensify over time on ASCs grown on pure Fg scaffolds from 7 to 21 days in culture (Figure 4D–4F). Fg scaffolds seeded with ASCs maintained with control media for 21 days showed little if any ARS staining at 21 days of culture (Figure 4C). We observed that bone-induced samples of ASC-seeded Fg scaffolds hardened and became physically brittle only when seeded with ASCs (not with BJs or BMSCs), with the created discs (~80–120 μ m thick) proving too fragile for consistent mechanical testing.

ASC Osteoblastogenesis on Electrospun Fg

To further assess ASC and BMSC osteoblastogenesis with electrospun Fg scaffolds, quantitative RT-PCR (qRT-PCR) was conducted to assess expression levels of Runx2, alkaline phosphatase (AP), and osteocalcin, which are markers of early, mid, and late stages of osteoblastogenesis, re-

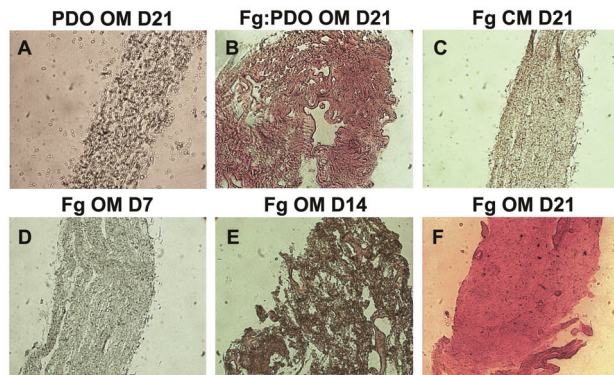


Figure 4: Mineralization of Electrospun PDO, Fg:PDO, and Fg Scaffolds. Alizarin Red S (ARS) staining of ASCs grown in osteogenic media (OM) for 21 days on electrospun PDO (A) and 50:50 Fg:PDO (B) indicate scaffold mineralization for only the 50:50 blend. Pure Fg scaffold with ASCs grown in control media (CM) lacked ARS staining at 21 days of culture (C), while ARS staining increases with time on pure Fg scaffolds seeded with ASCs in osteogenic media at 7 (D), 14 (E), and 21 days (F) of differentiation.

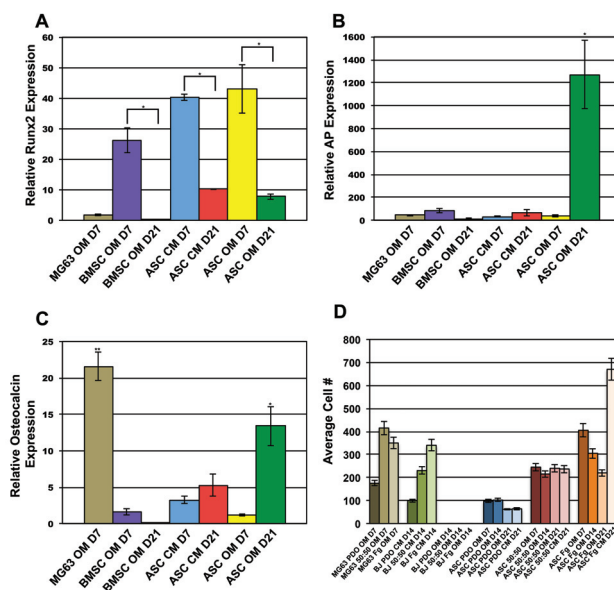


Figure 5: Gene Expression of ASCs and BMSCs on Electrospun Fg and Cell Counts. (A) Quantitative RT-PCR shows Runx2 expression at 1 week vs. 3 weeks of culture in both osteogenic media (OM) and control media (CM) for ASCs grown on Fg scaffolds. qRT-PCR analysis of alkaline phosphatase (AP) (B) and osteocalcin (C) gene expression from ASCs on pure Fg, in either CM or OM at 7 or 21 days of culture, is shown. MG63 cells serve as a positive control for osteocalcin expression. (D) The average cell number was also quantified on the different Fg and Fg:PDO scaffold types with CM or OM from 7–21 days of culture, as indicated. *indicates statistical significance at $p < 0.05$ vs. 18S housekeeping control using one-way ANOVA followed by a Tukey's test for pairwise comparisons. **indicates statistical significance at $p < 0.05$ over all groups (except MG63).

spectively (Figure 5). A substantial increase of Runx2 expression was noted in ASCs in osteogenic media (OM) but also in control media (CM) at 7 weeks of culture on Fg scaffolds (Figure 5A). AP gene expression at 3 weeks of differentiation was markedly increased compared to 1 week of differentiation only for ASCs seeded on Fg, while controls and ASCs showed no significant changes out to 3 weeks in osteogenic or control media (Figure 5B). Only ASCs in osteogenic media seeded on pure electrospun Fg scaffolds at 3 weeks of differentiation showed significant upregulation of osteocalcin relative to 1 week of differentiation (Figure 5C), while the MG63 positive osteoblast control cells showed high osteocalcin gene expression on Fg scaffolds, as expected (Figure 5C). Consistent with the Ki-67 staining (see Figure 1E), we observe a decline in cell number during differentiation of ASCs on both pure Fg and Fg:PDO blend that is not observed in control media (Figure 5D).

To determine if mature bone proteins were being synthesized and incorporated into the electrospun Fg matrix, osteocalcin expression of bone-induced ASCs on electrospun Fg was assessed using immunofluorescence and confocal microscopy after 3 weeks of culture. Figure 6 shows a mild fiber auto-fluorescence in each panel, slightly obscuring the signal; however, the osteocalcin immunolabeling intensity is clearly observed above background levels and is observed extracellularly in bone-induced scaffolds on pure Fg and Fg:PDO blended scaffolds (Figure 6), which was detectable in cell seeded scaffolds maintained in control media (not shown). In prior studies in our laboratory, osteocalcin staining was also confirmed with ASCs grown on plastic in osteogenic media, with strong positive staining in bone-induced cells observed both microscopically and validated by Western blotting to validate the antibody quality (data not shown).

4 Discussion

While direct comparisons of osteoblastogenesis models to actual bone regeneration *in vivo* have a variety of technical, logistical, and ethical challenges, we show here a practical *in vitro* replica of cell-matrix interaction-related events that mimic some of the key early events of bone regeneration, using a biomimetic approach for bone-related tissue engineering. As described in the early steps of actual bone regeneration, ASCs (and fibroblasts, as previously shown [34]) actively remodel the electrospun Fg by depositing new type I collagen, the predominant organic component of bone. We observed that ASCs (of a putative pericyte origin) can infiltrate the Fg, undergo osteoblasto-

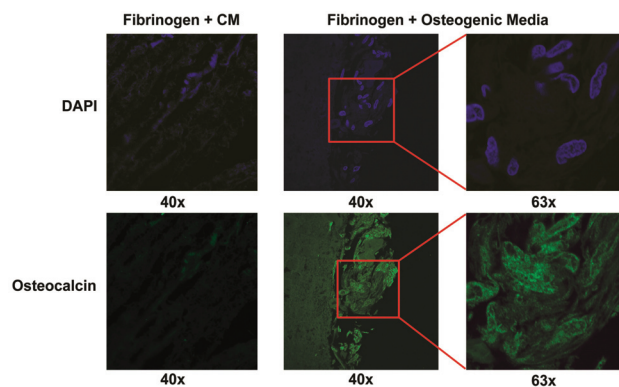


Figure 6: Osteocalcin Protein Expression in Osteo-Induced ASCs on Electrospun Fg. ASCs were seeded on electrospun Fg and cultured for 21 days in osteogenic media (OM). Sections of ASC/Fg were immunostained for osteocalcin along with a nuclear DAPI stain. ASCs grown on Fg in control media (CM) for 21 days (left panels) showed minimal staining, while the inclusion of no primary antibody in the immunostaining served as a negative control for osteocalcin staining (not included). Magnification is as indicated. (Note: mild autofluorescence from the nanofibers is also observed in all groups at the same exposure level).

genesis, and synthesize new collagen, as found in actual bone fracture repair from periosteum or pericytes.

Electrospinning produces scaffolds highly amenable to cell adhesion, viability, and osteogenic differentiation using many different template scaffold materials [26, 38]. The electrospinning of Fg nanofibers, published first by Wnek *et al.* [27], has provided a tissue engineering approach with extensive research and therapeutic potential. However, prior publications with electrospun Fg matrix lacked mechanical stability to serve as tissue engineering scaffolds without crosslinking, as the Fg scaffolds completely dissociated in 1–2 weeks of culture, a problem consistently observed with electrospun collagen scaffolds [38]. While the mechanical properties of electrospun Fg may be augmented by chemical crosslinking, we have previously reported that chemical crosslinking inhibits cell growth and differentiation [37]. Blending Fg with a synthetic polymer, such as PDO, improves scaffold stability in media [33, 37]. We show here that ASCs inherently possess a unique ability to remodel a sustainable scaffold in long-term culture. For up to 75 days of culture with uncrosslinked Fg, ASCs produced a cellularized Fg scaffold composed of new collagen (and likely other ECM materials) with long-term *in vitro* stability.

We find that electrospun Fg and Fg:PDO scaffolds are capable of supporting the proliferation of ASCs *in vitro* as noted by positive Ki67 staining and increased cell number over time. In contrast, during osteoblastogenesis, we observed a decline in both mitotic activity and cell num-

ber as ASCs differentiate in osteogenic media, indicating that ASCs may be exiting the cell cycle and fully committing to osteoblast differentiation. Interestingly, our model osteoblast cell line (MG63) completely destroys the electrospun Fg matrix in as little as 3 days, likely the result of high levels of metalloproteinases (MMPs) reportedly produced by MG63 cells, as some MMPs are known to regulate fibrin-invasion [39].

Synthetic materials are valued in tissue engineering because of their mechanical strength, their elastic properties, and their general thrift and abundance relative to naturally derived materials. Unfortunately, synthetic materials tend to have poor cell-matrix interactions, as we show here, and often are reactive with the host immune system. The typically poor cellular response of synthetic polymers can be improved by the addition of natural materials, as shown previously with pre-osteoblast cells grown in electrospun polycaprolactone (PCL)/hydroxyapatite matrices [40]. Similarly, we show that the typical poor cell-attachment response, low proliferation and scaffold penetration, and poor osteogenic potential of a synthetic material, PDO, can be enhanced by the addition of a natural protein, Fg.

It is becoming well established that cell-ECM dynamics play roles in cell fate determination, gap-junction communications, cell alignment and shape modulation, gene expression, cytoskeletal organization, and other functions using many different cell types [41, 42]. Osteoblastogenesis is a process highly dependent on chemical, structural, and mechanical interactions with ECM components, where, for example, ordered type I collagen fibrils are essential for regulating osteoblast differentiation from osteoprogenitors [43]. The ECM can also stimulate circulating and resident stem cells and bone precursor cells for regeneration by way of local niche elements [44]. Prior studies suggest that electrospun PCL fibers either coated with calcium phosphate or co-electrospun with collagen, relative to PCL fibers alone, are capable of stimulating osteoblastogenesis with commonly used MC3T3-E1 osteoprecursor cells [45, 46]. The ability of a scaffold to maintain and induce differentiation may be a critical parameter of an ideal scaffold for therapeutic use. Additional work also suggests that type I collagen formed as biomimetic electrospun nanofibers is able to support osteoblastogenesis, and in some ways, model bone regeneration *in vitro*, with a strong biomimetic response favoring collagen fibers over collagen films for upregulating osteogenic differentiation [38]. The earliest stage of bone regeneration, however, involves fibrin clot formation before collagen deposition.

In a model system mimicking native cell-ECM features of early-stage bone regeneration *in vivo*, we show elec-

trospun Fg nanofibers support ASC attachment, proliferation, scaffold remodeling and matrix mineralization. Using a biomimetic approach, we present an *ex vivo* model of osteoblastogenesis with multiple cellular and matrix components (Table 1, column 2) recapitulating bone fracture healing *in vivo* (Table 1, column 1). The pairing of ASCs and Fg-based electrospun fibers may provide an entirely autologous therapeutic strategy that is amenable to adding additional ECM and cellular constituents associated with bone regeneration events *in vivo*. Thus, we present a model that will be a valuable tool for further elucidating cell-matrix interactions critical for proper bone regeneration.

Acknowledgement: Thanks to Dr. Scott Henderson for expert confocal imaging analysis support, to Judy Williamson for SEM discussion, and especially to Dr. Jorge Almenara and the VCU Clinical Pathology Research Services. This study was supported in part by the VCU Department of Pathology (S.E.H. and L.W.E.), the VCU Department of Human and Molecular Genetics (S.E.H.), K01CA105050 (L.W.E.) from the National Cancer Institute, and W81XWH-09-1-0500 (L.W.E.) from the Department of Defense Breast Cancer Research Program. The content is solely the responsibility of the authors and does not necessarily represent the official views of the National Cancer Institute or the National Institutes of Health.

References

- [1] Lieberman J.R., Friedlaender G.E. (2005), Bone regeneration and repair: biology and clinical applications. Humana Press, ISBN-10: 0896038475
- [2] Schindeler A., McDonald M.M., Bokko P., Little D.G. (2008), Bone remodeling during fracture repair: The cellular picture. *Semin Cell Dev Biol* 19:459–66.
- [3] Liebschner M.A.K., Wettergreen M.A. (2003), Optimization of Bone Scaffold Engineering for Load Bearing Applications. Topics in Tissue Engineering, Eds. Ashammakhi N, Ferretti P.
- [4] Valbonesi M. (2006), Fibrin glues of human origin. *Best Pract Res Clin Haematol.* 19:191–203
- [5] Ho S.T., Huttmacher D.W., Ekaputra A.K., Hitendra D., Hui J.H. (2010), The evaluation of a biphasic osteochondral implant coupled with an electrospun membrane in a large animal model. *Tissue Eng Part A* 16:1123–41.
- [6] Zimmermann R., Jakubietz R., Jakubietz M., Strasser E., Schlegel A., Wiltfang J., Eckstein R. (2001), [Different preoperation method to obtain platelet components as a source of growth factors for local application.](#) *Transfusion* 41:1217–1224.
- [7] Ho W., Tawil B., Dunn J.C.Y., Wu B.M. (2006), The behavior of human mesenchymal stem cells in 3D fibrin clots: Dependence on fibrinogen concentration and clot structure. *Tissue Engineering* 12:1587–1595.
- [8] Catelas I., Sese N., Wu B.M., Dunn J.C.Y., Helgerson S., Tawil B. (2006), [Human Mesenchymal Stem Cell Proliferation and Osteogenic Differentiation in Fibrin Gels in Vitro.](#) *Tissue Engineering* 12:2385–2396.
- [9] Bensaïd W., Triffitt J.T., Blanchat C., Oudina K., Sedel L., Petite H. (2003), [A biodegradable fibrin scaffold for mesenchymal stem cell transplantation.](#) *Biomaterials* 24:2497–502.
- [10] Isogai N., Landis W.J., Mori R., Gotoh Y., Gerstenfeld L., Upton J., Vacanti J. (2000), Experimental Use of Fibrin Glue to Induce Site-Directed Osteogenesis from Cultured Periosteal Cells. *Plast Reconstr Surg* 105:953–63.
- [11] Lendeckel S., Jödicke A., Christophis P., Heidinger K., Wolff J., Fraser J.K., Hedrick M.H., Berthold L., Howaldt H.P. (2004), [Autologous stem cells \(adipose\) and fibrin glue used to treat widespread traumatic calvarial defects: case report.](#) *J Craniomax Surg* 32:370–3.
- [12] Zuk P.A., Zhu M., Mizuno H., Huang J., Futrell J.W., Katz A.J., Benhaim P., Lorenz H.P., Hedrick M.H. (2001), Multilineage cells from human adipose tissue: implications for cell-based therapies. *Tissue Eng* 7:211–28.
- [13] Zuk P.A., Zhu M., Ashjian P., De Ugarte D.A., Huang J.L., Mizuno H., Alfonso Z.C., Fraser J.K., Benhaim P., Hedrick M.H. (2002), [Human adipose tissue is a source of multipotent stem cells.](#) *Mol Biol Cell* 13:4279–95.
- [14] Katz A.J., Tholpady A., Tholpady S.S., Shang H., Ogle R.C. (2005), [Cell surface and transcriptional characterization of human adipose-derived adherent stromal \(hADAS\) cells.](#) *Stem Cells* 23:412–23.
- [15] Izadpanah R., Trygg C., Patel B., Kriedt C., Dufour J., Gimble J.M., Bunnell B.A. (2006), [Biologic properties of mesenchymal stem cells derived from bone marrow and adipose tissue.](#) *J Cell Biochem* 99:1285–97.
- [16] Kern S., Eichler H., Stoeve J., Klüter H., Bieback K. (2006), Comparative analysis of mesenchymal stem cells from bone marrow, umbilical cord blood, or adipose tissue. *Stem Cells* 24:1294–301.
- [17] Chamberlain G., Fox J., Ashton B., Middleton J. (2007), Concise review: mesenchymal stem cells: their phenotype, differentiation capacity, immunological features, and potential for homing. *Stem Cells* 25:2739–49.
- [18] Wang M., Crisostomo P.R., Herring C., Meldrum K.K., Meldrum D.R. (2006), Human progenitor cells from bone marrow or adipose tissue produce VEGF, HGF, and IGF-I in response to TNF by a p38 MAPK-dependent mechanism. *Am J Physiol Regul Integr Comp Physiol* 291:R880–4.
- [19] Abedin M., Tintut Y., Demer L.L. (2004), [Mesenchymal stem cells and the artery wall.](#) *Circ Res* 95:671–676.
- [20] Amos P.J., Shang H., Bailey A.M., Taylor A., Katz A.J., Peirce S.M. (2008), [IFATS collection: The role of human adipose-derived stromal cells in inflammatory microvascular remodeling and evidence of a perivascular phenotype.](#) *Stem Cells* 26:2682–2690.
- [21] Crisan M., Yap S., Casteilla L., Chen C.W., Corselli M., Park T.S., Andriolo G., Sun B., Zheng B., Zhang L., Norotte C., Teng P.N., Traas J., Schugar R., Deasy B.M., Badyaluk S., Buhring H.J., Giacobino J.P., Lazzari L., Huard J., Péault B. (2008), A perivascular origin for mesenchymal stem cells in multiple human organs. *Cell Stem Cell* 3:301–313.
- [22] Traktuev D.O., Merfeld-Clauss S., Li J., Kolonin M., Arap W., Pasqualini R., Johnstone B.H., March K.L. (2008), A population of multipotent CD34-positive adipose stromal cells share pericyte and mesenchymal surface markers, reside in a periendothelial

- location, and stabilize endothelial networks. *Circ Res* 102:77–85.
- [23] Zannettino A.C., Paton S., Arthur A., Khor F., Itescu S., Gimble J.M., Gronthos S. (2008), [Multipotential human adipose-derived stromal stem cells exhibit a perivascular phenotype in vitro and in vivo](#). *J Cell Physiol* 214:413–421.
- [24] Barnes C.P., Sell S.A., Boland E.D., Simpson D.G., Bowlin G.L. (2007), [Nanofiber technology: designing the next generation of tissue engineering scaffolds](#). *Adv Drug Deliv Rev* 59:1413–33.
- [25] Boland E.D., Coleman B.D., Barnes C.P., Simpson D.G., Wnek G.E., Bowlin G.L. (2005), [Electrospinning polydioxanone for biomedical applications](#). *Acta Biomater* 1:115–23.
- [26] Venugopal J., Low S., Choon A.T., Kumar T.S.S., Ramakrishna R. (2008), [Mineralization of osteoblasts with electrospun collagen/hydroxyapatite nanofibers](#). *J Mater Sci Mater Med* 19:2039–46.
- [27] Wnek G.E., Carr M., Simpson D.G., Bowlin G.L. (2003), [Electrospinning of nanofiber fibrinogen structures](#). *Nano Lett* 3:213–216.
- [28] Francis M.P., Sachs P.C., Madurantakam P.A., Sell S.A., Elmore L.W., Bowlin G.L., Holt S.E. (2012), [Electrospinning Adipose Tissue-Derived Extracellular Matrix for Adipose Stem Cell Culture](#). *J Biomed Mat Res Part A* 100:1716–24.
- [29] Mosesson M.W. (2005), [Fibrinogen and fibrin structure and functions](#). *J Thromb Haemost* 3:1894–904.
- [30] Giannini G., Mauro V., Agostino T., Gianfranco B. (2004), [Use of autologous fibrin platelet glue and bone fragments in maxillofacial surgery](#). *Transfus Apheresis Sci* 30:139–144.
- [31] McManus M.C., Boland E.D., Simpson D.G., Barnes C.P., Bowlin G.L. (2007), [Electrospun fibrinogen: feasibility as a tissue engineering scaffold in a rat cell culture model](#). *J Biomed Mat Res A* 81:299–309.
- [32] McManus M., Boland E., Sell S., Bowen W., Koo H., Simpson D.G., Bowlin G.L. (2007), [Electrospun nanofibre fibrinogen for urinary tract tissue reconstruction](#). *Biomed Mat* 2:257–262.
- [33] McManus M.C., Boland E.D., Koo H.P., Barnes C.P., Pawlowski K.J., Wnek G.E., Simpson D.G., Bowlin G.L. (2006), [Mechanical properties of electrospun fibrinogen structures](#). *Acta Biomater* 2:19–28.
- [34] Francis M.P., Sachs P.C., Elmore L.W., Holt S.E. (2010), [Isolating adipose-derived mesenchymal stem cells from lipoaspirate blood and saline fraction](#). *Organogenesis* 6:10–14.
- [35] Sachs P.C., Francis M.P., Brumelle J., Rao R.R., Elmore L.W., Holt S.E. (2012), [Defining essential stem cell characteristics in adipose-derived stromal cells extracted from distinct anatomical sites](#). *Cell Tissue Res* 349:505–15.
- [36] Friedenstein A.J., Deriglasova U.F., Kulagina N.N., Panasuk A.F., Rudakowa S.F., Luria E.A., Ruadkow I.A. (1974), [Precursors for fibroblasts in different populations of hematopoietic cells as detected by the in vitro colony assay method](#). *Exp Hematol* 2:83–92.
- [37] Sell S.A., Francis M.P., Garg K., McClure M.J., Simpson D.G., Bowlin G.L. (2008), [Cross-linking methods of electrospun fibrinogen scaffolds for tissue engineering applications](#). *Biomed Mater* 3:045001 (11pp).
- [38] Sefcik L.S., Neal R.A., Kaszuba S.N., Parker A.M., Katz A.J., Ogle R.C., Botchwey E.A. (2008), [Collagen nanofibres are a biomimetic substrate for the serum-free osteogenic differentiation of human adipose stem cells](#). *J Tissue Eng Regen Med* 2:210–20.
- [39] Hotary K.B., Yana I., Sabeih F., Li X.Y., Holmbeck K., Birkedal-Hansen H., Allen E.D., Hiraoka N., Weiss S.J. (2002), [Matrix metalloproteinases \(MMPs\) regulate fibrin-invasive activity via MT1-MMP-dependent and -independent processes](#). *J Exp Med* 195:295–308.
- [40] Wutticharoenmongkol P., Pavasant P., Supaphol P. (2007), [Osteoblastic phenotype expression of MC3T3-E1 cultured on electrospun polycaprolactone fiber mats filled with hydroxyapatite nanoparticles](#). *Biomacromolecules* 8:2602–10.
- [41] Kim H.W., Yu H.S., Lee H.H. (2008), [Nanofibrous matrices of poly\(lactic acid\) and gelatin polymeric blends for the improvement of cellular responses](#). *J Biomed Mater Res A* 87:25–32.
- [42] McBeath R., Pirone D.M., Nelson C.M., Bhadriraju K., Chen C.S. (2004), [Cell shape, cytoskeletal tension, and RhoA regulate stem cell lineage commitment](#). *Devel Cell* 6:483–495.
- [43] Franceschi R.T., Iyer B.S. (1992), [Relationship between collagen synthesis and expression of the osteoblast phenotype in Mc3t3-E1 cells](#). *J Bone Miner Res* 7:235–246.
- [44] Shih Y.R., Chen C.N., Tsai S.W., Wang Y.J., Lee O.K. (2006), [Growth of mesenchymal stem cells on electrospun type I collagen nanofibers](#). *Stem Cells* 24:2391–2397.
- [45] Mavis B., Demirtaş T.T., Gümüşderelioglu M., Gündüz G., Colak U. (2009), [Synthesis, characterization and osteoblastic activity of polycaprolactone nanofibers coated with biomimetic calcium phosphate](#). *Acta Biomater* 5:3098–3111.
- [46] McCullen S.D., Zhu Y., Bernacki S.H., Narayan R.J., Pourdeyhimi B., Gorga R.E., Lobo E.G. (2009), [Electrospun composite poly\(L-lactic acid\)/tricalcium phosphate scaffolds induce proliferation and osteogenic differentiation of human adipose-derived stem cells](#). *Biomed Mater* 4:035002 (9pp).